

Degeneracy in the characterization of non-transiting planets from transit timing variations

G. Boué^{1,2*}, M. Oshagh^{1,3}, M. Montalto¹, and N. C. Santos^{1,3}

¹*Centro de Astrofísica, Universidade do Porto, Rua das Estrelas, 4150-762 Porto, Portugal*

²*ASD, IMCCE-CNRS UMR8028, Observatoire de Paris, UPMC, 77 avenue Denfert-Rochereau, 75014 Paris, France*

³*Departamento de Física e Astronomia, Faculdade de Ciências, Universidade do Porto, Portugal*

Accepted Received ...; in original form ...

ABSTRACT

The transit timing variation (TTV) method allows the detection of non-transiting planets through their gravitational perturbations. Since TTVs are strongly enhanced in systems close to mean-motion resonances (MMR), even a low mass planet can produce an observable signal. This technique has thus been proposed to detect terrestrial planets. In this letter, we analyse TTV signals for systems in or close to MMR in order to illustrate the difficulties arising in the determination of planetary parameters. TTVs are computed numerically with an n -body integrator for a variety of systems close to MMR. The main features of these TTVs are also derived analytically. Systems deeply inside MMR do not produce particularly strong TTVs, while those close to MMR generate quasiperiodic TTVs characterised by a dominant long period term and a low amplitude remainder. If the remainder is too weak to be detected, then the signal is strongly degenerate and this prevents the determination of the planetary parameters. Even though an Earth mass planet can be detected by the TTV method if it is close to a MMR, it may not be possible to assert that this planet is actually an Earth mass planet. On the other hand, if the system is right in the center of a MMR, the high amplitude oscillation of the TTV signal vanishes and the detection of the perturber becomes as difficult as it is far from MMR.

Key words: Planets and satellites: detection – Planetary systems – Celestial mechanics

1 INTRODUCTION

A transiting planet belonging to a multiplanetary system may suffer gravitational interactions. The perturbations in the orbit can then produce observable variations in the transit midtimes with respect to those of a purely Keplerian orbit. This is the basic idea behind the transit timing variation method which has been proposed to detect non-transiting terrestrial planets (Agol et al. 2005; Holman & Murray 2005).

The TTV signal scales roughly linearly with the mass of the perturber (Agol et al. 2005; Holman & Murray 2005; Nesvorný & Morbidelli 2008). Thus, low-mass planets generate weak TTVs except if they are in mean motion resonance or near period commensurability with the transiting planet (Agol et al. 2005; Holman & Murray 2005). In that case, the TTV signal contains a long term oscillation associated to a “great inequality”, as for the Jupiter-Saturn system (Lissauer et al. 2011; Ballard et al. 2011). This long

period, like all the oscillations in the TTV signal, scales linearly with the period of the transiting planet and is of the order of a year for a three-day transiting planet. Such systems, if they exist, should thus start to be detectable in surveys like CoRoT or Kepler. However, most of the systems close to MMR generate similar TTVs (Ford & Holman 2007), and many perturber parameters can reproduce an observed TTV signal (Nesvorný & Morbidelli 2008; Meschiari & Laughlin 2010; Veras et al. 2011). Such a difficulty has already been experienced with the Kepler 19 system (Ballard et al. 2011). Nevertheless, short-term perturbations, if detectable, should produce a “chopping signal” that raises the degeneracy (Holman et al. 2010).

Analytical expressions of the order of magnitude of the amplitude and the period of TTV signals for systems in or near first-order mean-motion resonances are provided by Agol et al. (2005). Here, we propose to focus on higher order resonances. In a first section, we compare the TTV signal produced by an Earth mass planet with typical detection thresholds to motivate the study of these resonances. In a second section, we present a few examples of TTV signals for

* E-mail: gwenael.boue@astro.up.pt

a variety of planetary parameters. In the subsequent section, we provide analytical approximations of the TTV signal for systems near or at MMR. We conclude in the last section.

2 TTV AMPLITUDE PRODUCED BY AN EARTH MASS PLANET

We consider the strength of TTVs produced by a terrestrial planet of mass $m_2 = M_\oplus$ on a Jupiter mass planet ($m_1 = M_J$) transiting a star with mass $m_0 = M_\odot$. The orbit of the transiting planet is assumed to be initially circular with a period $P_1 = 3$ days. Since second and higher order mean motion resonances only exist for non zero eccentricities, we set the eccentricity of the perturbing planet to $e_2 = 0.1$. The TTVs are computed using an n -body integrator over $N = 300$ transits which corresponds to 2.5 years. The system is supposed to be coplanar, the initial mean longitudes λ_1 , λ_2 of the two planets and the longitude of the periastris ϖ_2 of the perturber are arbitrarily set to 270 deg which is the direction of the observer.

The strength of TTVs is measured in the same way as in Agol et al. (2005), using the standard deviation

$$\sigma = \sqrt{\frac{1}{N} \sum_{j=1}^N (t_j - t_0 + P_1 j)^2}, \quad (1)$$

where P_1 and t_0 are chosen to minimize σ , and t_j , $j \geq 1$, are the midtransit times of the N transits. This quantity σ is displayed in figure 1 for 1000 different initial conditions evenly spread over the period P_2 of the perturber between $2P_1$ and $10P_1$. We recognize the well known peaks centered on period commensurabilities corresponding to amplified gravitational interactions (Agol et al. 2005; Holman & Murray 2005). The figure shows also the range of typical detection thresholds varying from 10 sec to 1 min depending on the instrument and on the depth of the transit. It is noteworthy that, for the system considered in this letter, terrestrial planets can hardly produce signals at the limit of detection and only in the vicinity of period commensurabilities with $P_2/P_1 \leq 3$. Since the amplitude of TTV scales linearly with the period of the transiting planet, the signal produced on a wider orbit, with a period ten times larger for instance, would be easier to detect. However, the period of the TTV signal would be ten times longer too. It may exceed the duration of the surveys like CoRoT and Kepler. With this choice of initial conditions, most of the systems do not enter MMR because the value of the resonant angle is that of the hyperbolic point (see section 4.2).

3 TTV SIGNAL NEAR A PERIOD COMMENSURABILITY

To illustrate the degeneracy of the TTV signal, we consider 8 different initial conditions, near different mean motion resonances. The system is the same as in the previous section, apart from the mass of the perturber m_2 and its eccentricity e_2 which are chosen so as to produce TTVs with the same amplitude (~ 2 min) and the same period (4 oscillations during the 2.5 years) for each of the different orbital periods P_2 . The initial conditions are gathered in Table 1. Although

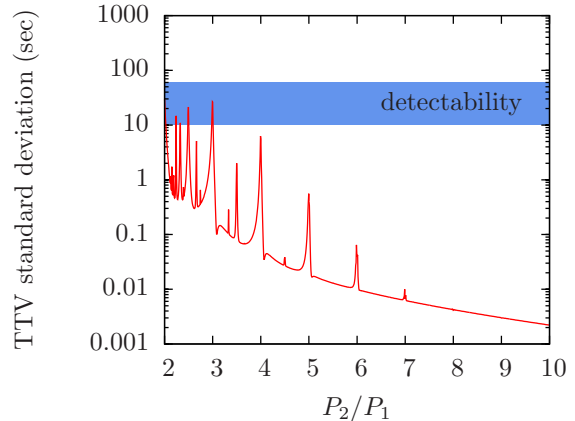


Figure 1. Standard deviation of TTVs produced by an Earth mass planet on a Jovian planet transiting a Solar mass star every three days. The stripe shows the range of typical detectability thresholds.

Table 1. Planetary parameters used to perform the simulations of the Figure 2.

set ^a	MMR	m_2 (M_\oplus)	e_2 ^b	ε	$\sqrt{\chi_r^2}$
1	1 : 2	0.9	0.087	0.0132	1.36
2	4 : 9	24.5	0.120	0.0034	1.15
3	3 : 7	21.1	0.100	0.0044	1.13
4	2 : 5	8.6	0.102	0.0067	1.02
5	3 : 8	17.2	0.160	0.0045	1.07
6	1 : 3	49.7	0.100	0.0134	1.25
7	3 : 10	95.2	0.194	0.0045	1.30
8	1 : 4	394.0	0.115	0.0134	1.31

^a The initial conditions are in order of increasing semi-major axis.

^b The eccentricity e_2 is chosen to produce low values of the reduced chi square $\sqrt{\chi_r^2}$.

this letter focuses on second and higher order period commensurabilities, we consider the 1:2 resonance to highlight the fact that even a 0.9 Earth mass planet can generate a TTV signal with the same amplitude and shape as a 4.14 Saturnian mass planet near the 1:4 resonance.

Figure 2 shows the TTV signals, computed for the 8 initial conditions of table 1, to which a gaussian noise with $\sigma_{\text{noise}} = 20$ seconds has been added to simulate observations. All the signals are very similar and easily detectable. But they are dominated by one single frequency and look like simple noisy sinusoids. It is thus quite difficult to differentiate them. For each signal, the highest amplitude sinusoid is extracted using a frequency analysis (Laskar 1990, 1993), and represented by a white curve in Fig. 2. Then, the reduced chi-square of this fit is computed and shown in the last column of the table 1. In all cases, the fit by a pure sine leads to a reduced chi-square lower than or of the order of 1.30. Naturally, if the two planets transit, the degeneracy disappears because the resonance is known. Here, we focus only on non-transiting perturbers.

In the following we derive an analytical approximation of this highest amplitude sinusoidal term.

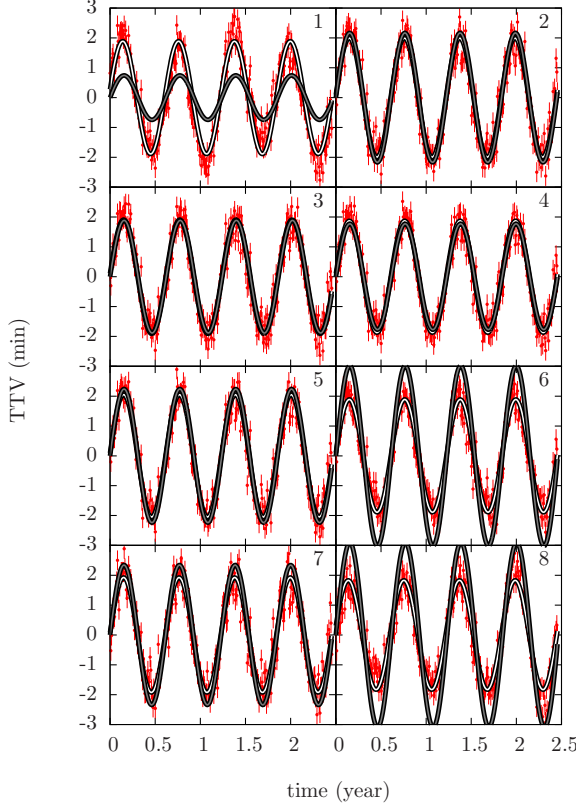


Figure 2. Example of TTV signal produced near period commensurabilities. A gaussian error of 20 seconds has been added to the signal to model the observation uncertainties. The white curve represents the highest amplitude term obtained by frequency analysis. The gray curve is the analytic approximation Eq. (21). The number at the upper right corner of each subfigure corresponds to the set of initial conditions as given in table 1.

4 ANALYTICAL APPROXIMATION OF THE HIGHEST AMPLITUDE TERM

We consider a coplanar system in the vicinity of the $p : p + q$ mean motion resonance. We assume that the orbit of the transiting planet is initially circular, while that of the perturber is eccentric. We define a_i , λ_i , e_i , ϖ_i as the semi-major axis, the mean longitude, the eccentricity and the longitude of pericenter of the i th planet, respectively. The conjugated variable to the mean longitude λ_i is, up to the first order in planet masses, $\Lambda_i = m_i \sqrt{G m_0 a_i}$ with G being the gravitational constant. The index $i = 1$ stands for the inner (transiting) planet, and the index $i = 2$ refers to the outer perturber. For each orbital parameter E_i , we note the unperturbed part \bar{E}_i , and the oscillatory perturbation δE_i such that $E_i = \bar{E}_i + \delta E_i$. For the system analysed in this section, the terms contributing to the transit timing variations δt of the inner planet are (e.g. Nesvorný & Morbidelli 2008)

$$n_1 \delta t = \delta \lambda_1 + 2\delta k_1 \sin(\bar{\lambda}_1) - 2\delta h_1 \cos(\bar{\lambda}_1) + \mathcal{O}(e_1). \quad (2)$$

In this expression, $n_1 = 2\pi/P_1$, defined by $Gm_0 = n_1^2 a_1^3$, is the mean motion of the transiting planet. $k_1 = e_1 \cos \varpi_1$ and $h_1 = e_1 \sin \varpi_1$ are the usual non-singular eccentricity variables of the transiting planet. With the convention $\lambda_1 = 3\pi/2$ at transit, Eq. (2) becomes

$$n_1 \delta t = \delta \lambda_1 - 2\delta k_1 + \mathcal{O}(e_1). \quad (3)$$

The Hamiltonian \mathcal{H} governing the evolution of a coplanar two-body system can be decomposed into a Keplerian part

$$\mathcal{H}_0 = -\frac{Gm_0 m_1}{2a_1} - \frac{Gm_0 m_2}{2a_2}, \quad (4)$$

and an interaction \mathcal{H}_1 given by

$$\mathcal{H}_1 = -\frac{Gm_1 m_2}{a_2} \sum_{\mathbf{j}, \mathbf{l}} C_{\mathbf{j}}^{\mathbf{l}}(\alpha) e_1^{\mathbf{l}_1} e_2^{\mathbf{l}_2} \times \cos(j_1 \lambda_1 + j_2 \lambda_2 + j_3 \varpi_1 + j_4 \varpi_2), \quad (5)$$

where $\alpha = a_1/a_2$. $C_{\mathbf{j}}^{\mathbf{l}}(\alpha)$ with $\mathbf{j} = (j_1, j_2, j_3, j_4)$ and $\mathbf{l} = (l_1, l_2)$ are coefficients that can be computed either in terms of Laplace coefficients $b_{s/2}^{(k)}(\alpha)$ (e.g. Ellis & Murray 2000), or through a series in power of α (e.g. Kaula 1962).

Here, we make the assumption that the evolution of a system in the vicinity of the $p : p + q$ MMR is well recovered when only the resonant terms with the lowest power in eccentricity are kept in Eq. (5). This is verified if the resonances are well separated (Wisdom 1980). One gets

$$\mathcal{H}_1 \simeq -e_2^q H_1 \cos(p\lambda_1 - (p+q)\lambda_2 + q\varpi_2) - e_1 e_2^{q-1} H_2 \cos(p\lambda_1 - (p+q)\lambda_2 + \varpi_1 + (q-1)\varpi_2) \quad (6)$$

where $H_i = 2Gm_1 m_2 C_i(\alpha)/a_2$ and

$$C_1(\alpha) = C_{(p, -p-q, 0, q)}^{(0, q)}(\alpha), \quad C_2(\alpha) = C_{(p, -p-q, 1, q-1)}^{(1, q-1)}(\alpha). \quad (7)$$

The factor 2 in the definition of H_i comes from the symmetry $C_{\mathbf{j}}^{\mathbf{l}}(\alpha) = C_{-\mathbf{j}}^{\mathbf{l}}(\alpha)$. In (6), we consider only the linear terms in e_1 as the higher orders do not contribute to the equations of motion for $\bar{e}_1 = 0$. Since the eccentricity e_2 does not enter in the expression of δt (3), we make the hypothesis that e_2 and its longitude of pericenter ϖ_2 are dominated by their constant (initial) value for the period of time considered in this study. Thus, e_2 and ϖ_2 are not variables, but just parameters of the problem. Hereafter, we note them \bar{e}_2 and $\bar{\varpi}_2$, respectively.

The evolution dictated by the resonant Hamiltonian, Eqs. (4) and (6), is obtained after applying the following conical transformation on the mean longitudes

$$\phi = -\lambda_1/(p+q), \quad (8)$$

$$\psi = p\lambda_1 - (p+q)\lambda_2 + q\varpi_2,$$

and on their conjugated momenta

$$\Phi = -(p+q)\Lambda_1 - p\Lambda_2, \quad (9)$$

$$\Psi = -\Lambda_2/(p+q).$$

In the new variables, the Hamiltonian reads

$$\tilde{\mathcal{H}}(\psi, \Phi, \Psi, h_1, k_1) = \tilde{\mathcal{H}}_0(\Phi, \Psi) - \bar{e}_2^q \tilde{H}_1(\Phi, \Psi) \cos \psi - \bar{e}_2^{q-1} \tilde{H}_2(\Phi, \Psi) (k_1 \cos(\psi - \bar{\varpi}_2) - h_1 \sin(\psi - \bar{\varpi}_2)). \quad (10)$$

It should be stressed that k_1 and h_1 are not conical variables. However, in the limit of vanishing eccentricity e_1 , the equations of motions are greatly simplified

$$\begin{aligned} \dot{\phi} &= \frac{\partial \tilde{\mathcal{H}}}{\partial \Phi}, & \dot{\psi} &= \frac{\partial \tilde{\mathcal{H}}}{\partial \Psi}, & \dot{k}_1 &= \frac{1}{\Lambda_1} \frac{\partial \tilde{\mathcal{H}}}{\partial h_1}, \\ \dot{\Phi} &= -\frac{\partial \tilde{\mathcal{H}}}{\partial \phi}, & \dot{\Psi} &= -\frac{\partial \tilde{\mathcal{H}}}{\partial \psi}, & \dot{h}_1 &= -\frac{1}{\Lambda_1} \frac{\partial \tilde{\mathcal{H}}}{\partial k_1}. \end{aligned} \quad (11)$$

Since the Hamiltonian (10) is independent of the cyclic variable ϕ , its conjugated momentum $\bar{\Phi}$ is constant. In the following, we assume, as in Wisdom (1980), that the functions $\tilde{H}_i(\Phi, \Psi)$, $i = 1, 2$ of the interaction part are well approximated by $\tilde{H}_i(\Phi, \bar{\Psi})$, where $\bar{\Psi} = \langle \Psi \rangle$ is the averaged value of Ψ .

4.1 Outside of MMR

Outside of the $p : p + q$ MMR, we assume that the Keplerian Hamiltonian $\tilde{\mathcal{H}}_0(\Phi, \Psi)$ is sufficiently well approximated by the linear term in its Taylor series about $\Psi = \bar{\Psi}$. In that case, the resonant Hamiltonian (10) becomes

$$\tilde{\mathcal{H}} \simeq \tilde{\mathcal{H}}_0(\Phi, \bar{\Psi}) + \left. \frac{\partial \tilde{\mathcal{H}}_0}{\partial \Psi} \right|_{\Psi=\bar{\Psi}} (\Psi - \bar{\Psi}) - \bar{e}_2^q \tilde{H}_1(\Phi, \bar{\Psi}) \cos \psi - \bar{e}_2^{q-1} \tilde{H}_2(\Phi, \bar{\Psi}) (k_1 \cos(\psi - \bar{\omega}_2) - h_1 \sin(\psi - \bar{\omega}_2)), \quad (12)$$

with,

$$\tilde{H}_i(\Phi, \bar{\Psi}) = 2\bar{\Lambda}_1 n_1 \frac{m_2}{m_0} \bar{\alpha} C_i(\bar{\alpha}), \quad (13)$$

for $i = 1, 2$, and

$$\left. \frac{\partial \tilde{\mathcal{H}}_0}{\partial \Psi} \right|_{\Psi=\bar{\Psi}} \equiv \omega_\psi(\Phi, \bar{\Psi}) = pn_1 - (p + q)n_2 = \pm pn_1 \varepsilon. \quad (14)$$

In (14), the parameter ε , which cancels out at the resonance, is a measure of the closeness to the exact resonance. Its expression is

$$\varepsilon = \left| 1 - \frac{p + q}{p} \frac{n_2}{n_1} \right|. \quad (15)$$

For infinitely small eccentricity e_1 , the evolution of ψ and Ψ governed by the Hamiltonian (12) is independent of k_1 and h_1 . Using (11), one finds

$$\begin{aligned} \psi(t) &= \psi(0) + \omega_\psi(\Phi, \bar{\Psi})t, \\ \Psi(t) &= \Psi(0) + \frac{\tilde{H}_1(\Phi, \bar{\Psi})}{\omega_\psi(\Phi, \bar{\Psi})} \bar{e}_2^q (\cos \psi(t) - \cos \psi(0)). \end{aligned} \quad (16)$$

To get the evolution of ϕ , we assume that $\partial \tilde{\mathcal{H}} / \partial \Phi$ is well approximated by the linear expansion of $\partial \tilde{\mathcal{H}}_0 / \partial \Phi$ about $\Psi = \bar{\Psi}$, whose the expression reads

$$\frac{\partial \tilde{\mathcal{H}}_0}{\partial \Phi} = -\frac{n_1}{p + q} + 3 \frac{pn_1}{p + q} \frac{\Psi - \bar{\Psi}}{\Lambda_1}. \quad (17)$$

Integrating (17) with $\bar{\Psi} = \langle \Psi(t) \rangle$, one gets

$$\begin{aligned} \phi(t) &= \phi(0) - \frac{n_1 t}{p + q} \\ &+ 3 \frac{pn_1}{p + q} \frac{\tilde{H}_1(\Phi, \bar{\Psi})}{\omega_\psi(\Phi, \bar{\Psi})^2} \frac{\bar{e}_2^q}{\Lambda_1} (\sin \psi(t) - \sin(\psi(0))). \end{aligned} \quad (18)$$

From the equations of change of variables (8), using the expression of $\tilde{H}_1(\Phi, \bar{\Psi})$, Eq. (13), $\omega_\psi(\Phi, \bar{\Psi})$, Eq. (14), and removing the linear terms in (18), one obtains

$$\delta \lambda_1 = -\frac{6}{p} \frac{m_2}{m_0} \frac{\bar{\alpha} C_1(\bar{\alpha})}{\varepsilon^2} \bar{e}_2^q \sin \psi(t). \quad (19)$$

The expression of δk_1 is obtained from the integration of the equations of motion (11) of the Hamiltonian (12). After removing the linear terms, the result is

$$\delta k_1 = \mp \frac{2}{p} \frac{m_2}{m_0} \frac{\bar{\alpha} C_2(\bar{\alpha})}{\varepsilon} \bar{e}_2^{q-1} \cos(\psi(t) - \bar{\omega}_2). \quad (20)$$

From the expressions (19) and (20), one can see that the ratio between the amplitudes of $\delta \lambda_1$ and δk_1 is of the order of \bar{e}_2 / ε . Thus, for a system sufficiently close to a MMR, $\varepsilon \lesssim \bar{e}_2$, the amplitude of the TTV signal (3) is dominated by $\delta \lambda_1$. In that case,

$$\delta t \simeq -\frac{6}{pn_1} \frac{m_2}{m_0} \frac{\bar{\alpha} C_1(\bar{\alpha})}{\varepsilon^2} \bar{e}_2^q \sin \psi(t). \quad (21)$$

The period of the dominant sinusoidal oscillation in the TTV signal $P = 2\pi / |\omega_\psi(\Phi, \bar{\Psi})|$ is related to the period of the transiting planet by (see Eq. (14))

$$P = \frac{1}{p\varepsilon} P_1. \quad (22)$$

This relation has been inverted to compute the distance ε from each resonance in the different simulations of the section 3, see table 1.

The analytical approximation of TTVs (21) is plotted as gray curves for each numerical experiment in Fig. 2. The agreement with the numerical simulations is very good except for the largest distances to MMR: $\varepsilon \sim 1.30$. Nevertheless, the order of magnitude of the amplitude is still correct within a factor 2.

4.2 Inside of MMR

The reasoning is the same as in the case outside of MMR. The only difference is that the linear terms in the Taylor series of $\tilde{\mathcal{H}}_0(\Phi, \Psi)$ about $\Psi = \bar{\Psi} = \Psi_{\text{res}}$ is zero. Thus, we expand $\tilde{\mathcal{H}}_0(\Phi, \Psi)$ up to the quadratic order as in Wisdom (1980). Furthermore, we neglect the contribution δh_1 in the TTV, as in the previous subsection. The part proportional to $\tilde{H}_2(\Phi, \Psi_{\text{res}})$ is thus removed from the Hamiltonian. We get

$$\begin{aligned} \tilde{\mathcal{H}} &= \tilde{\mathcal{H}}_0(\Phi, \Psi_{\text{res}}) + \frac{1}{2} \left. \frac{\partial^2 \tilde{\mathcal{H}}_0}{\partial \Psi^2} \right|_{\Psi=\Psi_{\text{res}}} (\Psi - \Psi_{\text{res}})^2 \\ &- \bar{e}_2^q \tilde{H}_1(\Phi, \Psi_{\text{res}}) \cos \psi \end{aligned} \quad (23)$$

with

$$\frac{1}{2} \left. \frac{\partial^2 \tilde{\mathcal{H}}_0}{\partial \Psi^2} \right|_{\Psi=\Psi_{\text{res}}} = -\frac{3}{2} \frac{p^2 n_1}{\Lambda_1} \frac{m_1 + \bar{\alpha} m_2}{\bar{\alpha} m_2}. \quad (24)$$

The Hamiltonian (23) is that of a pendulum. The center of libration depends on the sign of $\tilde{H}_1(\Phi, \Psi_{\text{res}})$. If it is positive, as in most of the cases, the libration is around $\psi = \psi_{\text{res}} = \pi$, otherwise it is around $\psi_{\text{res}} = 0$. Since the initial conditions used for the simulations in section 3 ($\lambda_1 = \lambda_2 = \bar{\omega}_2 = 270$ deg) imply $\psi(0) = 0$, most of the resonances have been crossed at the hyperbolic point. To study the TTV inside of a MMR, we thus change the initial conditions, and take $\lambda_2 = 90$ deg. The other parameters are those of the set 3 in the table 1.

To get the evolution of $\phi(t)$, and then $\delta \lambda_1(t)$, one should note that the oscillating term in $\dot{\phi} = \partial \tilde{\mathcal{H}} / \partial \Phi$ (17) is proportional to $(\Psi - \Psi_{\text{res}})$ which is also proportional to $\dot{\psi} = \partial \tilde{\mathcal{H}} / \partial \Psi$. One obtains

$$\begin{aligned} \phi(t) &= \phi(0) - \frac{n_1 t}{p + q} \\ &+ \frac{3}{\Lambda_1} \frac{pn_1}{p + q} \left(\left. \frac{\partial^2 \tilde{\mathcal{H}}_0}{\partial \Psi^2} \right|_{\Psi=\Psi_{\text{res}}} \right)^{-1} (\psi(t) - \psi(0)). \end{aligned} \quad (25)$$

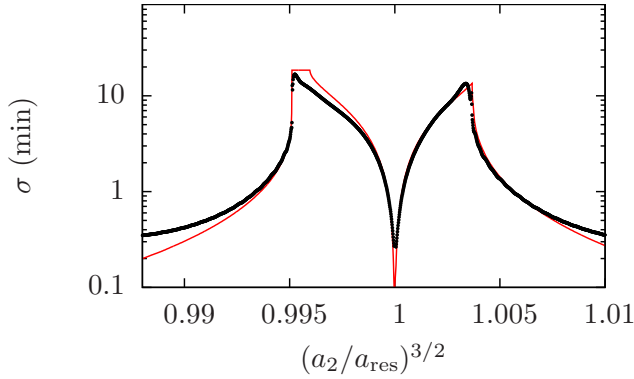


Figure 3. Detail of the TTV amplitude through the 3 : 7 MMR. The initial conditions are those of the set 3 (Tab. 1) with the initial mean longitude $\lambda_2 = 90$ deg. Each black point corresponds to a different initial semi-major axis a_2 of the perturber. The thin solid line corresponds to the analytical formulae (21), (27) taking into account the amplitude of libration $\Delta\psi$ inside the resonance. The amplitude of libration is computed from the initial conditions using the relation $\tilde{\mathcal{H}}(\psi(0), \Psi(0)) = \tilde{\mathcal{H}}(\psi_{\text{res}} \pm \Delta\psi, \Psi_{\text{res}})$ where $\tilde{\mathcal{H}}$ is the resonant Hamiltonian (23).

Removing the linear part of (25), and using Eqs. (8), (24), one finds

$$\delta\lambda_1 = \frac{1}{p} \frac{\bar{\alpha}m_2}{m_1 + \bar{\alpha}m_2} (\psi(t) - \psi_{\text{res}}). \quad (26)$$

The corresponding TTV expression (3) is

$$\delta t = \frac{1}{pn_1} \frac{\bar{\alpha}m_2}{m_1 + \bar{\alpha}m_2} (\psi(t) - \psi_{\text{res}}). \quad (27)$$

This expression is similar to that given by Agol et al. (2005) for first order MMR. In (27), the resonant angle ψ is librating. So, the absolute value of $(\psi(t) - \psi_{\text{res}})$ is bounded by the amplitude of libration, which is also bounded by π .

Figure 3 shows the evolution of the dispersion σ (1) of the TTV signal for systems in the vicinity the 3 : 7 MMR. The analytical approximation plotted as a solid curve is given by (21) outside of the MMR, and by (27) inside of the MMR, within $(a_2/a_{\text{res}})^{3/2} \simeq 0.995$ and 1.004 . In both cases, the analytical values are divided by $\sqrt{2}$ to convert amplitudes into dispersions. Outside of the MMR, the dispersion is larger for systems closer to the separatrices. This is due to the factor $1/\varepsilon^2$ in (21). Inside of the MMR, the dispersion of TTV is also larger towards the separatrices, but the reason is different (Veras et al. 2011). Inside MMR, the dispersion is proportional to the amplitude of libration which is maximal at the separatrices.

For completeness, we provide also the libration frequency ω_{lib} at the center of resonant islands. This is an upper limit of the frequency of the highest amplitude oscillation in TTV signals. Indeed, closer to the separatrices, the period gets longer. The expression of this frequency is

$$\begin{aligned} \omega_{\text{lib}} &= \sqrt{\left| \bar{e}_2^q \tilde{\mathcal{H}}_1(\Phi, \Psi_{\text{res}}) \left(\frac{\partial^2 \tilde{\mathcal{H}}_0}{\partial \Psi^2} \Big|_{\Psi=\Psi_{\text{res}}} \right) \right|} \\ &= pn_1 \sqrt{6 \left(\bar{\alpha} \frac{m_2}{m_0} + \frac{m_1}{m_0} \right) |C_1(\bar{\alpha})| \bar{e}_2^q}. \end{aligned} \quad (28)$$

5 CONCLUSION

A terrestrial planet at a period ratio larger than 2 with a Jovian transiting planet may produce detectable TTV only if the system is at resonance, but not in the exact center, or near period commensurability. If a system is sufficiently close to a second or higher order resonance, to be detected, then the TTV signal is dominated by a sinusoidal oscillation which is difficult to distinguish from one resonance to another. Moreover, the derived analytical approximations of TTV signals Eqs. (21) and (27) show that once the main period P of the TTV is known, the amplitude still depends on the mass m_2 , the eccentricity e_2 , and the period P_2 (through the semi-major axis ratio $\bar{\alpha}$) of the perturber. The problem is thus highly degenerate. The examples presented in this letter show that an Earth mass planet is able to produce a signal comparable to that produced by a Saturn mass planet. We thus conclude that the TTV method may benefit from radial velocity observations in order to characterize non-transiting planets.

ACKNOWLEDGEMENTS

This work was supported by the European Research Council/European Community under the FP7 through Starting Grant agreement number 239953. We also acknowledge the support from Fundação para a Ciência e a Tecnologia (FCT) through program Ciência2007 funded by FCT/MCTES (Portugal) and POPH/FSE (EC), and in the form of grant reference PTDC/CTE-AST/098528/2008.

REFERENCES

- Agol E., Steffen J., Sari R., Clarkson W., 2005, MNRAS, 359, 567
- Ballard S., Fabrycky D., Fressin F., Charbonneau D., Desert J.-M., et al. 2011, ArXiv e-prints
- Ellis K. M., Murray C. D., 2000, Icarus, 147, 129
- Ford E. B., Holman M. J., 2007, ApJ, 664, L51
- Holman M. J., Fabrycky D. C., Ragozzine D., Ford E. B., Steffen J. H., et al. 2010, Science, 330, 51
- Holman M. J., Murray N. W., 2005, Science, 307, 1288
- Kaula W. M., 1962, AJ, 67, 300
- Laskar J., 1990, Icarus, 88, 266
- Laskar J., 1993, Physica D, 67, 257
- Lissauer J. J., Fabrycky D. C., Ford E. B., Borucki W. J., Fressin F., et al. 2011, Nature, 470, 53
- Meschiari S., Laughlin G. P., 2010, ApJ, 718, 543
- Nesvorný D., Morbidelli A., 2008, ApJ, 688, 636
- Veras D., Ford E. B., Payne M. J., 2011, ApJ, 727, 74
- Wisdom J., 1980, AJ, 85, 1122

This paper has been typeset from a \TeX / \LaTeX file prepared by the author.